ELSEVIER

Materials Science and Engineering A 493 (2008) 48–52

MATERIALS SCIENCE & ENGINEERING A

www.elsevier.com/locate/msea

Influence of grain size on orientation changes during plastic deformation

S. Scheriau *, R. Pippan

Christian Doppler Laboratory for Local Analysis of Deformation and Fracture, Erich Schmid Institute of Materials Science, Austrian Academy of Sciences, Jahnstrasse 12, 8700 Leoben, Austria

Received 19 February 2007; received in revised form 4 June 2007; accepted 29 August 2007

Abstract

Polycrystalline copper, nickel and iron with grain sizes of 100 μm, 10 μm, 1 μm and about 100 nm were deformed in an in situ deformation stage installed in a scanning electron microscope to study the influence of grain size on orientation changes during plastic deformation. By using the electron back scatter diffraction technique, the microstructural evolution and the crystallographic orientation rotation behaviour taking place during tensile deformation were investigated at three different deformation steps. On the basis of the captured data, domains near grain boundaries show different orientation changes as compared to the inner region of a grain, especially in samples with grains larger than 10 μm. At grain sizes smaller than 1 μm, this distinctive difference between the near grain boundary region and the interior of grains disappears. In summary, it could be shown that orientation changes in grains larger than 1 μm differ significantly from the behaviour in submicrometer and nanocrystalline materials.

Keywords: EBSD; Orientation changes; SPD; In situ deformation

1. Introduction

Formability as well as mechanical properties of metals and alloys exhibit a strong dependence on grain size and grain structure. Despite the vast number of studies on the effect of grain size on the deformation behaviour and the developed substructure [12,13], the controlling processes are not fully understood. Many different techniques have been applied – e.g. X-ray diffraction (XRD), transmission electron microscopy (TEM) – to analyse changes in crystal textures, variations of dislocation densities or to depict selected elements of the developed substructure at a certain strain [14]. Electron back scatter diffraction (EBSD) offers a new tool to study the local evolution of the substructure and microtexture during the deformation experiments [2,3,7,8,10].

In this analysis microstructural evolutions and crystallographic orientation rotation behaviour taking place during tensile deformation at room temperature were investigated in polycrystalline iron, nickel and copper. Special attention is devoted to possible differences in nano and microcrystalline materials. Tensile test specimens were deformed in an in situ deformation stage installed in a scanning electron microscope that is equipped with an EBSD system. Variations in surface and grain boundary characteristics, such as surface deformation, misorientation, and dislocation distribution, that evolve during the in situ deformation, were examined using both scanning electron microscope (SEM) images and EBSD maps. The orientation changes in individual grains were traced at three different deformation steps while the evolution of the sample surface was studied during the whole deformation process.

2. Experimental procedure

Measurements on the crystal orientation were carried out with an EBSD-SEM system, a TSL EBSD system interfaced to a LEO 1525.

The analysed materials were polycrystalline nickel, iron and copper; the chemical analysis is given in Table 1.

At first the initial material was severely deformed in a high-pressure torsion (HPT) process [4,6,11]. The samples with a diameter of 14 mm and a thickness of 2 mm were deformed to 3200%. This huge strain corresponds to a steady state where no further refinement of the crystallites takes place. Such kind of deformation leads to the evolution of an ultrafine and even nano-sized grain structure. However, the resulting small crystallites produced by severe plastic deformation (SPD) contain a huge

* Corresponding author.
E-mail addresses: scheriau@unileoben.ac.at (S. Scheriau), pippan@unileoben.ac.at (R. Pippan).

0921-5093/$ – see front matter © 2007 Elsevier B.V. All rights reserved.
doi:10.1016/j.msea.2007.08.092

Table 1
Chemical contents of the analysed material (wt.%)

	Cu	Al	Si	Fe	Mn	Mg	Zn	Te
Cu	>99,99	0,0002	0,0002	0,0016	0,0014	0,0009	0,0013	0,0001
	Ni	Co	Cu	Fe	C	S		
Ni	>99,97	$5x10^{-5}$	0,001	0,0015	<0,10	0,0003		
	Fe	C	Mn	Al	N	S	P	
Fe	>99,98	0,0016	0,0095	0,0031	0,0034	<0,0005	<0,0005	

amount of stored energy in the form of dislocations in their processed state [5,9]. Thereby these dislocations are not randomly distributed. They accumulate in grain like boundaries, which separate regions with a lower dislocation density.

After this severe deformation, the material was exposed to a heat treatment process so that grains start to coarsen. By interrupting this recrystallization or grain growth process after a defined time, samples with a mean microstructural size of 100 μm, 10 μm, 1 μm and 300 nm were fabricated. Out of these samples tensile test specimens were machined by milling. Fig. 1 shows a sketch of two tension specimens.

To remove damaged and oxidized surface regions, the machined tensile samples with a gauge length of 6.2 mm and a cross section of $1.2 \times 1\,mm^2$ were polished mechanically as well as electro-chemically.

To trace the orientation changes and the evolution of the surface characteristics always in the same area of the specimen, thin cuts were made with a focused ion beam (FIB) at two positions on the surface of the polished tensile sample. To capture the grain orientations of the undeformed state an EBSD scan was taken at 0% elongation. In the same way, scans at 7% and 20% local plastic deformation were taken to study the orientation changes of individual grains inside the area limited by the FIB marks. The specimen was then strained at room temperature using a Kammrath and Weiss in situ deformation stage, which was installed in the scanning electron microscope. At deformation steps of 2%, 5%, 7%, 12%, 16% and 20%, high resolution SEM images were taken to determine the local plastic deformation and to chase the processes taking place on the surface. It should be noted that EBSD only shows the orientation changes in the very near surface region. In [2] it was shown that for strains smaller than 20%, the observed changes in the crystal orientation of the near surface and the interior of grains are very similar.

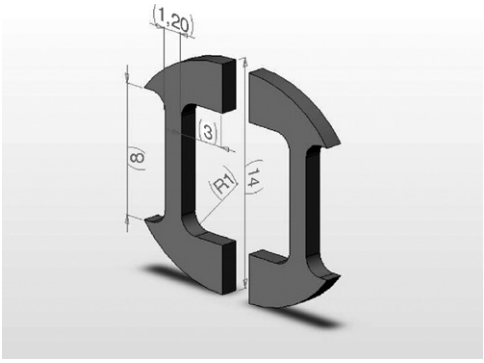

Fig. 1. Tensile test samples fabricated out of a HPT disc.

3. Results

The SEM images in Fig. 2a and c illustrate the surface of a copper tensile sample with a grain size of about 100 μm before and after deformation. They show the evolution of the surface morphology during elongation up to a plastic deformation of 20%. On the same sample EBSD measurements were performed exactly in the region that is limited by the FIB marks (dashed lines). In Fig. 2b and d, two inverse pole figure (IPF) maps show the orientation changes during uniaxial tensile deformation; the serrations at the grain boundaries in the maps are caused by the coarse step size. Each colour corresponds according to the standard triangle to a specific crystallographic orientation.

As seen in Fig. 2, the grains show a single orientation in the unstrained state. A distinctive feature of the SEM images is that the occurring slip lines run straight through the grain and get curved at grain boundaries. Throughout the whole grain structure, geometrically necessary dislocations, which cause the orientation changes, are installed to ensure the coherence along the grain boundaries. At 20% plastic deformation the onset of a fragmentation into domains with different orientation could be observed.

With increasing strain a change in the crystallographic orientation can be measured. This variation in the orientation inside a grain and near grain boundaries is caused by dislocations generated during the plastic deformation and arranged in diffuse networks. As the level of plastic deformation is increased, the number and density of stored and pinned dislocations raise up, leading to an intense change in the crystal orientations within a grain (see Fig. 2d).

At very small grain sizes, a significant change in crystal orientation inside a grain is hardly observed, especially at grain sizes smaller than 1 μm. In Fig. 3, two EBSD maps are depicted for nickel with a mean microstructural size of 200 nm. The sample was strained up to a local plastic deformation of 12%. Both maps belong to different positions on the sample surface. Because of the surface contamination, it is not possible to catch two maps from the same position.

Due to a small extent of hardening in fine grained material, the deformation inside grains is less than in a coarse grained material. To get more quantitative information about the magnitude of orientation changes, pole figure maps were calculated at each deformation step using the orientation-imaging microscopy software. By using EBSD, the information comes from a small region near the surface by just including some grains. But it is possible to have a closer look on the local lattice rotation of individual grains during straining.

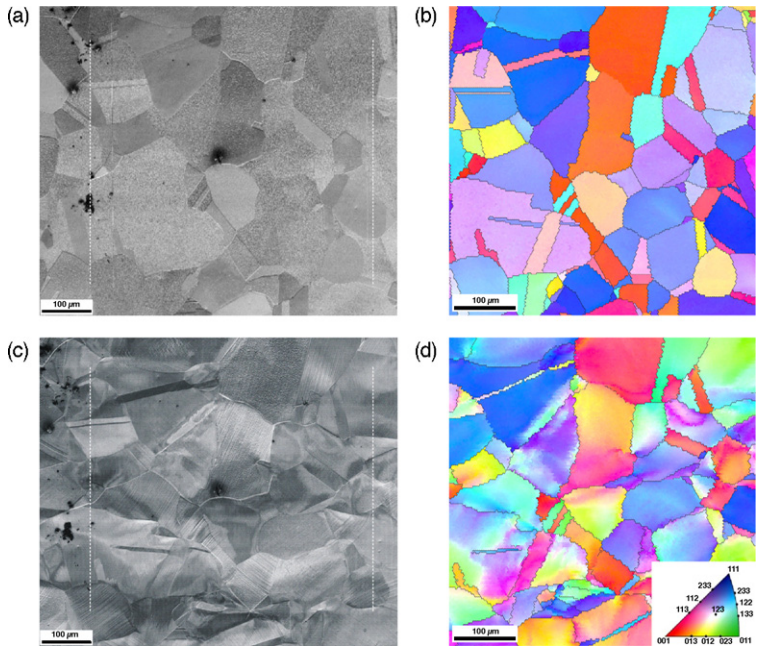

Fig. 2. SEM images on the (left) and EBSD maps on the (right) captured from the surface of the 100 μm grain sized Cu specimen before (top, 0%) and after (bottom, 20%) deformation; standard triangle used for the EBSD maps.

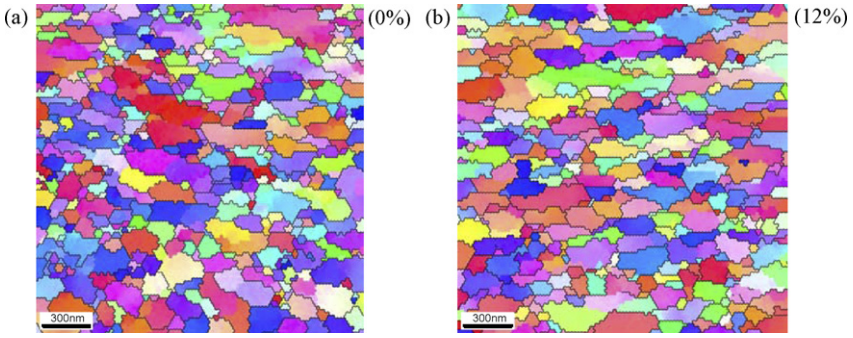

Fig. 3. EBSD maps for nickel with a mean microstructural size of 200 nm: (a) undeformed state, (b) sample strained up to 12% local plastic deformation. See text for further details.

There is a relatively large dispersion of crystal orientation of highly deformed specimen, despite the small number of grains present in the map. In the undeformed state the measured points are tightly clustered around the genuine crystal orientation corresponding to a selected grain. Clearly the plastic deformation has caused the points to spread from the central orientation due to the low angle rotations of local crystal regions. In Fig. 4, two pole figure maps for nickel are shown. In Fig. 4a the pole figure was calculated for an average grain size of 100 μm and a local plastic deformation of 20%. The typical broadening in orientation of highly deformed samples comes out clearly, especially for grains larger than 10 μm. By dropping the grain size below 1 μm, this large dispersion disappears. In Fig. 4b, the calculated pole figure belongs to an average grain size of about 200 nm. The sample was strained up to 12% plastic deformation where fracture appears. No dis-

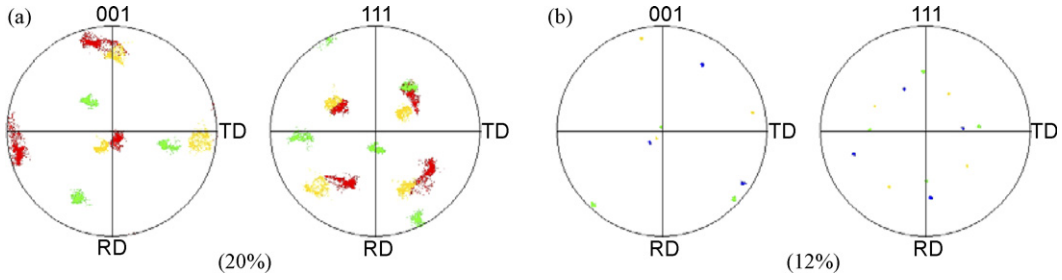

Fig. 4. Pole figures of selected grains of nickel calculated for two different grain sizes: 100 μm (left) and 200 nm (right); the numbers in brackets indicate the amount of deformation.

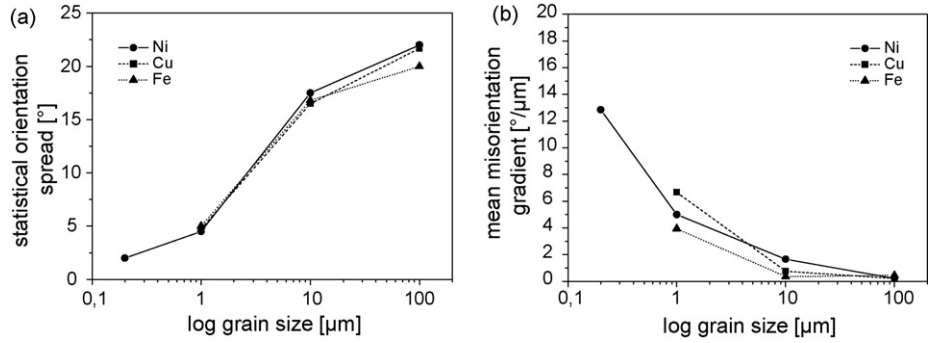

Fig. 5. Statistical orientation spread (°) and mean misorientation gradient (°/μm) as a function of grain size at 20% plastic deformation.

tinctive orientation spread of highly deformed grains could be observed.

The magnitude of the broadening in the crystal orientation from the central orientation was quantified. Fig. 5 shows two graphs for the calculated crystal dispersions; because of the recrystallization of Cu and the brittle behaviour of Fe, only limited data is shown for grains smaller than 1 μm. In most grains the change of the mean orientation is relatively small. As the deformation proceeds the initial orientation of a single grain increasingly spreads around the genuine positions in the pole figure maps. Fig. 5a reflects the low-angle rotations of local crystal regions. For grains larger than 10 μm the statistical spread was found to be settled around 18–22°, whereas for grains smaller than 1 μm this value drops below 5°. In Fig. 5b, the mean misorientation gradient based on line profiles in the IPF maps was plotted versus the logarithm of the grain size. It is clearly evident that the misorientation gradient (MG) inside a grain is the highest for the smallest grain size. With increasing grain size, the MG decreases rapidly and was found to be the lowest for the largest grains. This seems to be surprising; however, one should take into account that despite the higher MG in the very small grains the developed misorientation inside is significantly smaller.

4. Discussion

By comparing the data on the influence of grain size on the orientation changes during plastic deformation, one can identify two regimes: regime I with an average grain size, $d_a > 1$ μm and regime II with $d_a < 1$ μm. The deformation structure in regime I is characterised by the onset of the fragmentation of coarse grains into domains with different orientation. In regime II, where the grain size is below 1 μm, the taken EBSD maps do not show the formation of such substructures. The transition from regime I to regime II occurs in all three investigated materials at an average grain size of about 1 μm.

In regime I orientation changes occur throughout the whole grain because in different regions of a single grain different slip systems are activated, which is induced by the variation of the local stresses. There is reasonable agreement between SEM images and IPF maps taken. At the boundaries between the different slip regions, the generated dislocations are partly stored and a misorientation is built up between these regions. With increasing strain the misorientation increases and a further subdivision takes place.

In regime II the formation of domains below an average grain size of 1 μm could not be seen in the scanning electron microscope. According to the micrographs, taken during the tensile test, no slip lines could be detected on the sample surface [1]. Even the IPF maps of highly deformed tension samples show no orientation fluctuations inside the small grains. A misorientation comes up only at the vicinity of grain boundaries for samples with a grain size of about 1 μm [1]. It seems that in these grains only one group of slip systems are activated and dislocations are able to pass through the grain. A pile up of dislocations is given primarily at high angle grain boundaries, which is responsible for the observed misorientation.

In the materials with a grain size of about 200 nm, it seems that the pile up consumes nearly the whole grain (see Fig. 3 or [1]). Due to the small grain size the grains are filled up with dislocations of the same Burgers vector but they do not form a substructure (not visible in the SEM). The deformation seems to be realised by the movement of dislocations from grain boundaries to grain boundaries.

By comparison of the collected data of Fe, Ni and Cu, all materials showed a similar behaviour in the evolution of domains with different orientation [1]. Thereby the aforementioned process is not affected by the crystal structure (bcc or fcc).

5. Conclusions

Tension samples of polycrystalline copper, nickel and iron were strained at ambient temperature up to 20% local plastic deformation. The mechanisms taking place during tensile testing were investigated especially focusing on the evolving orientation changes that come up inside deformed grains. The detailed analysis of the collected data has shown that:

(i) Plastic deformation strongly depends on the grain size and grain structure. Thus, orientation changes taking place during tensile tests appear quite inhomogeneous.
(ii) Depending on the governing deformation mechanisms, two regimes were identified. Regime I, $d > 1$ μm, is controlled by the activation of different slip systems in different

regions of a grain. The fragmentation of a single grain into domains with different orientation dominates the structural evolution of deformed grains.

(iii) In regime II, $d < 1\,\mu m$, the interaction of different slip systems inside a grain and the fragmentation of a single grain into domains with different orientation could not be observed. It seems that dislocations move from grain boundary to grain boundary leading to a high orientation gradient inside the grains.

References

[1] St. Scheriau, Diplomarbeit, Montanuniversität Leoben, 2005 http://www.oeaw.ac.at/esi/download/pdf/dipl/dipl-Scheriau-S.pdf.
[2] A. Musienko, A. Tatschl, K. Schmidegg, O. Koldenik, R. Pippan, G. Cailletaud, Acta Mater. 55 (2007) 4121.
[3] A. Vorhauer, T. Hebesberger, R. Pippan, Acta Mater. 51 (2003) 677.
[4] T. Hebesberger, H.P. Stüwe, A. Vorhauer, F. Wetscher, R. Pippan, Acta Mater. 53 (2005) 393.
[5] N. Hansen, R.F. Mehl, Metall. Mater. Trans. A 32 (2001) 2917.
[6] A. Vorhauer, R. Pippan, Scripta Mater. 51 (2004) 921.
[7] J. Han, D. Kim, K. Jee, K. Hwan Oh, Mater. Sci. Eng. A 387 (2004) 60.
[8] A. Tatschl, O. Kolednik, Mater. Sci. Eng. A 342 (2003) 152.
[9] M.J. Zehetbauer, J. Kohout, E. Schafler, F. Sachslehner, A. Dubravina, J. Alloys Compd. 378 (2004) 329.
[10] P.J. Hurley, F.J. Humphreys, Acta Mater. 51 (2003) 1087.
[11] Z. Ruslan, Valiev, V. Igor, Alexandrov, Ann. Chim.-Sci. Mater. 27 (2002) 3.
[12] C.Y. Yu, P.W. Kao, C.P. Chang, Acta Mater. 53 (2005) 4019.
[13] O. Wouters, W.P. Vellinga, R. Van Tijum, J.Th.M. de Hosson, Acta Mater. 53 (2005) 4043.
[14] Z.J. Li, A. Godfrey, Q. Liu, Acta Mater. 52 (2004) 149.